

# Spectral, photometric, and dynamic analysis of eight Draconid meteors

Jiří Borovička · Pavel Koten · Lukáš Shrbený ·  
Rostislav Štork · Kamil Hornoch

Received: date / Accepted: date

**Abstract** We analyzed spectra, trajectories, orbits, light curves, and decelerations of eight Draconid meteors observed from Northern Italy on October 8, 2011. Meteor morphologies of two of the meteors are also presented, one of them obtained with a high resolution camera. Meteor radiants agree with theoretical predictions, with a hint that some meteors may belong to the pre-1900 meteoroid trails. The spectra confirm that Draconids have normal chondritic composition of main elements (Mg, Fe, Na). There are, nevertheless, differences in the temporal evolution of Na line emission. The differences are correlated with the shapes of the light curves and the deceleration rates. Our data confirm that Draconids are porous conglomerates of grains, nevertheless, significant differences in the atmospheric fragmentation of cm-sized Draconids were found. Various textures with various resistance to fragmentation exist among Draconid meteoroids and even within single meteoroids.

**Keywords** Meteors · Meteoroids · Draconids · Comets · 21P/Giacobini-Zinner

## 1 Introduction

The Draconid meteor shower, almost unnoticeable in most years, produced intense meteor storms in 1933 and 1946 as well as outbursts in 1985 and 1998 (Jenniskens 2006) and moderate activity in some other years, e.g. 2005 (Campbell-Brown et al. 2006; Koten et al. 2007). The parent body of the shower is the Jupiter family comet 21P/Giacobini-Zinner. The mechanism of the outbursts is now well understood, which allowed the prediction of another outburst on October 8, 2011 (Jenniskens 2006; Vaubaillon et al. 2011; Maslov 2011). The outburst was successfully observed by a number of teams using various techniques (e.g. Kero et al. 2012; Tóth et al. 2012; Trigo-Rodríguez et al. 2013; Madiedo et al. 2013; Vaubaillon et al. 2013). Here we report the results of our simultaneous spectral, photometric, and dynamic observations of eight relatively bright Draconid meteors. We concentrate on determination of physical and chemical properties of the meteoroids. This is a continuation of our previous work (Borovička et al. 2007), where we analyzed one bright and six faint (with no spectral data) Draconids observed in 2005.

Jiří Borovička · Pavel Koten · Lukáš Shrbený · Rostislav Štork · Kamil Hornoch  
Astronomical Institute, Academy of Sciences, 251 65 Ondřejov Observatory, Czech Republic  
E-mail: jiri.borovicka@asu.cas.cz

**Table 1** Instruments used in this work.

	MAIA video	Suppl. video	Spectral video	HDV video	All-sky photo	Wide-field photo
Camera	GigE Vision	DFK31	Panasonic NVS88	Canon Legria HV40	Canon EOS 5D Mark II	Canon EOS 450D
Image intensifier	Mullard XX1332	Dedal 41	Mullard XX1332	–	–	–
Grating	–	–	600 grooves/mm	–	–	–
Lens	1.4/50	1.4/50	2/85	native	2.8/15	3.5/10
Resolution	776×582	1024×768	768×576	1920×1080	5616×3744	4272×2848
Frame rate	61.15	15	25	25	–	–
Exposure time, s	0.01635	0.0667	0.04	0.008	30	20
ISO	–	–	–	–	1600	1600
Field of view	50°	30°	30°	18×10°	180° diagonal	95×70°
Pixel scale <sup>a</sup> deg/pixel	0.106	0.044	0.048	0.0095	0.024	0.029
Limiting magnitude	+5	+4	+2	0	0	+1
Recording	PC	laptop	S-VHS tape	MiniDV tape	card	card
Site	A,B	A	B	B	B	A
Captured meteors	4,5,8 (A) 1–8 (B)	2–8	1–8	6	2,3,4,6	1,2,4–8

<sup>a</sup>in the center of the field

## 2 Instrumentation

Our observations were performed at two sites in Northern Italy, Brenna (site A, longitude 9.18795°, latitude 45.73371°, altitude 333 m) and Barengo (site B, 8.50505°, 45.56606°, 238 m). Both sites were equipped with high frame rate image intensified video cameras MAIA (Koten et al. 2011) for measuring meteor trajectories, velocities and light curves. The trajectory work was supported by one supplementary video on site A and one DSLR camera at each site. For studying meteor morphologies, a high-resolution (HDV format) non-intensified video camera was used for the first time. The shutter speed was set to 1/120 s, so that quasi-instantaneous images of the meteor could be taken. The camera had low sensitivity and small field of view, so the chances of capturing a meteor were not high. Nevertheless, one meteor was captured and its shape could be studied in much higher detail than with other cameras used.

The spectra were taken with our image intensified spectral video camera. We used longer focal length than usual to increase spectral resolution, at the cost of a smaller field of view. More details of our expedition to Italy and the observation strategy are given in our first report (Borovička et al. 2013). Technical details of the cameras are given in Table 1.

**Table 2** List of studied meteors.

#	Time UT	Mass g	$z_R$ °	$h_{\text{beg}}$ km	$h_{\text{max}}$ km	$M_{\text{max}}$ mag	$h_{\text{end}}$ km	Range km	$Q$ °
1	18:03:20	0.15	20.5	98	83.9	+0.7	82	145–133	34
2	18:20:00	2.3	22.1	107	93–90	−2.0	83	225–210	25
3	19:58:22	0.4	35.6	102	91–90, 88.3	−0.4	83.5	155–135	46
4	20:05:35	3.3	36.5	107.5	96–93	−2.3	80.5	176–146	30
5	20:19:34	0.4	38.7	101.5	89.6	0.0	84	125–104	2
6	20:28:21	2.7	39.9	105	82.8	−3.1	76.5	146–116	27
7	20:43:51	0.3	41.3	101	96–93.5	+0.3	86	185–170	15
8	20:55:34	0.1	43.3	99	98–93.5	+1.3	88.5	133–120	4

**Table 3** Pre-atmospheric velocities, geocentric radiant, geocentric velocities, and orbits of the observed meteors (equinox J2000.0).

#	$v_{\infty}$ km/s	$\alpha_G$ °	$\delta_G$ °	$v_G$ km/s	$a$ AU	$e$	$q$ AU	$\omega$ °	$i$ °	$\Omega$ °
1	23.44 ±.25	263.41 ±.29	55.49 ±.33	20.74 ±.28	3.48 ±.22	0.714 ±.018	0.9966 ±.0002	173.62 ±.23	31.46 ±.33	194.949
2	23.55 ±.25	263.29 ±.33	55.52 ±.40	20.88 ±.28	3.56 ±.24	0.720 ±.019	0.9965 ±.0002	173.54 ±.26	31.63 ±.34	194.960
3	23.20 ±.50	263.18 ±.25	55.66 ±.14	20.54 ±.57	3.28 ±.36	0.697 ±.033	0.9965 ±.0001	173.48 ±.21	31.30 ±.63	195.027
4	23.57 ±.15	263.16 ±.14	55.74 ±.10	20.96 ±.17	3.54 ±.13	0.719 ±.010	0.9964 ±.0001	173.50 ±.12	31.80 ±.19	195.032
5	23.48 ±.25	263.29 ±.28	55.96 ±.62	20.86 ±.28	3.42 ±.26	0.709 ±.022	0.9966 ±.0002	173.65 ±.24	31.76 ±.38	195.042
6	23.55 ±.15	262.93 ±.10	55.75 ±.10	20.95 ±.17	3.51 ±.12	0.716 ±.010	0.9963 ±.0001	173.33 ±.10	31.80 ±.19	195.048
7	23.38 ±.25	263.29 ±.19	55.52 ±.20	20.76 ±.28	3.47 ±.20	0.712 ±.017	0.9964 ±.0001	173.51 ±.15	31.49 ±.32	195.058
8	23.63 ±.40	263.04 ±.53	56.04 ±.3.8	21.04 ±.45	3.51 ±.1.2	0.716 ±.094	0.9964 ±.0008	173.49 ±.80	32.00 ±.1.4	195.066

### 3 Analyzed meteors

Eight Draconid meteor spectra were captured. All eight meteors were also observed by imaging cameras at both stations, so their trajectories could be computed. All meteor records listed in Table 1, except those from spectral and HDV cameras, were combined to compute the trajectories. Table 2 gives the basic data on the meteors, including their atmospheric trajectories. The time of appearance, photometric mass, zenith distance of the radiant,  $z_R$ , height of first registration,  $h_{\text{beg}}$ , height at maximum brightness,  $h_{\text{max}}$ , the absolute maximum brightness,  $M_{\text{max}}$ , height of disappearance,  $h_{\text{end}}$ , range to the camera, which was used to measure the light curve, and the convergence angle,  $Q$ , between the planes as seen from both sites are given. The photometric mass was computed using the luminous efficiency of Pecina and Ceplecha (1983). For meteors that exhibited flares, the height of maximum is given to 0.1 km. Conversely, the light curves of some meteors were flat near the maxima. In those cases a height range is given for the maximum. Meteor 3 had two maxima of equal brightness. The actual light curves are plotted in Fig. 1. The plane convergence angle was quite low for meteors 5 and 8, nevertheless, we were able to obtain relatively good trajectory solutions.

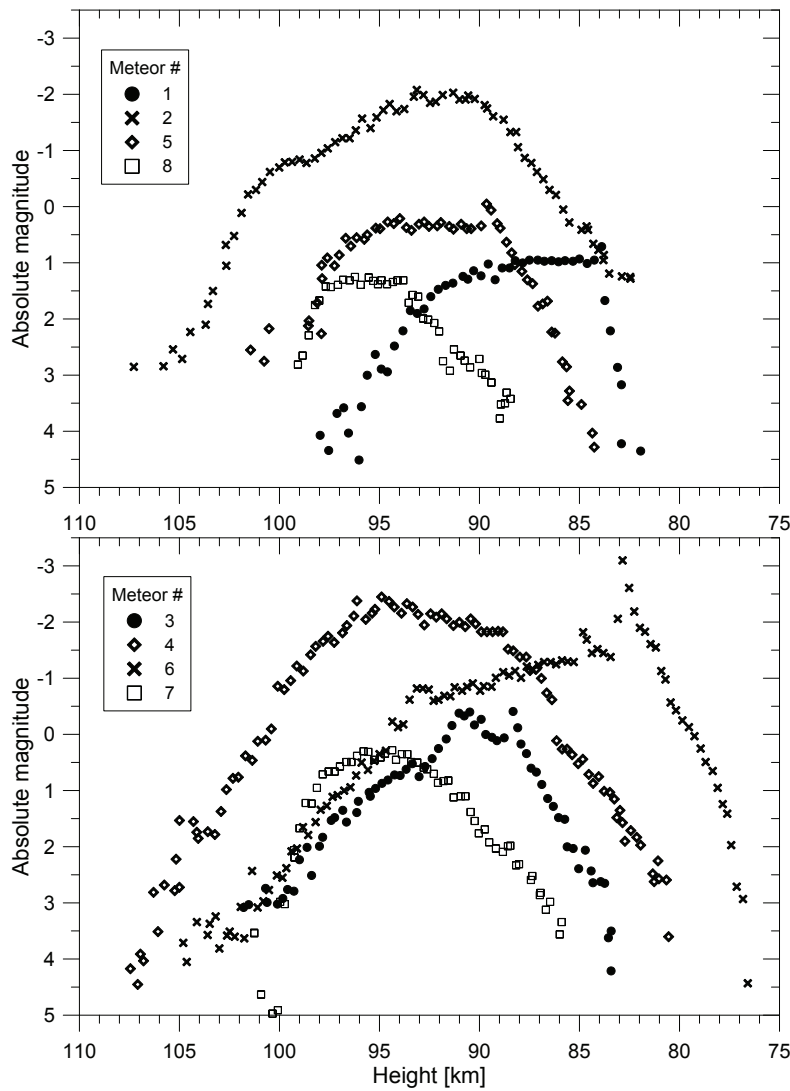


**Fig. 1** Meteor light curves as observed by the MAIA video cameras. The curves are presented in two plots to improve their visibility.

In Table 3, the initial velocity at the entry into the atmosphere,  $v_\infty$ , the geocentric radiant,  $\alpha_G$ ,  $\delta_G$ , geocentric velocity,  $v_G$ , and the orbital elements are given. The initial velocity was determined from the modeling of deceleration by the erosion model (Borovička et al. 2007). The error of the velocity was estimated from the spread of the measurements.

The geocentric radiants are plotted and compared with the results of other authors in Fig. 2. Our radiants show lower scatter than those of other authors and are close to the theoretical predictions (Maslov 2011; Vaubaillon et al. 2011). The meteors from the 1873–1894 trails were predicted to encounter the Earth earlier (about 17 UT) and to have radiants  $0.4^\circ$  to the South in comparison with the 1900 trail, which was responsible for the main

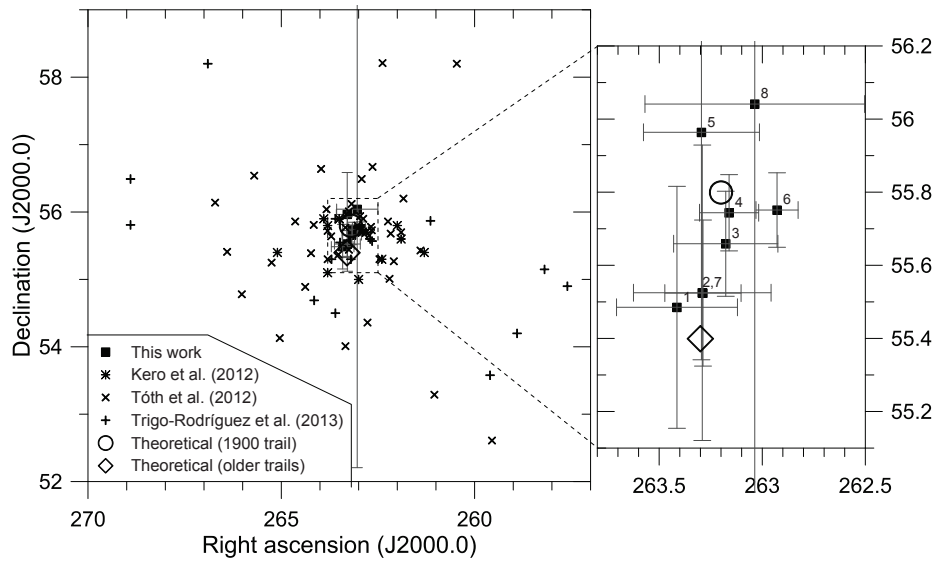


**Fig. 2** Geocentric radiants of 2011 Draconid meteors as observed by Kero et al. (2012), Tóth et al. (2012), Trigo-Rodríguez et al. (2013), and this work. Error bars are plotted for this work. Theoretical radiants predicted by J. Vaubaillon (<http://draconids.seti.org>) for the 1900 dust trail and 1873–1894 dust trails are given for comparison. The inset on the right shows our data in detail and with meteors identified.

activity peak around 20 UT. Judging from their time of appearance and radiant positions, it is possible that meteors 1 and 2 belonged to the older trails (see also Borovička et al. 2013). The most precise meteors 3, 4, and 6 almost certainly belonged to the 1900 trail.

#### 4 Spectra

The images of the four best spectra are reproduced in Fig. 3. The differences between meteor light curves shown in Fig. 1, are evident in these pictures. On the other hand, all spectra are similar with Mg and Na being the two brightest lines. The plot of the two best spectra, integrated over the duration of the meteors, is given in Fig. 4. The spectra contain significant continuous radiation over the whole wavelength range 3600–9000 Å. The continuum provides about half of the signal. N<sub>2</sub> molecular bands are also present. The reliably identified emission features are listed in Table 4. When corrected to the spectral sensitivity of the instrument, the blend of Fe and Mg lines near 3800 Å becomes another strong feature. If compared with the Leonids (Borovička et al. 1999), Draconids show lower intensities of the emissions of atmospheric origin (N, N<sub>2</sub>, O), which can be attributed to their much lower velocity in comparison to the Leonids. The lower velocity and lower intensity of atmospheric lines also favors the visibility of the low excitation lines of Na and K in the infrared (lines 19 and 21 in Table 4). They are seen in Draconids but not in Leonids. Otherwise, the meteoritic lines in Draconids are the same as seen in Leonids.

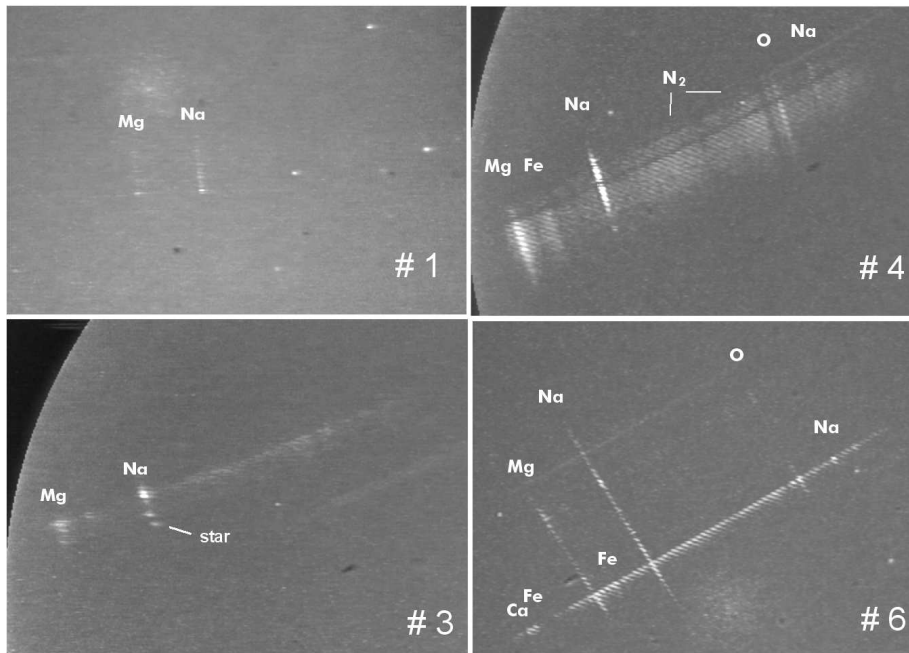


**Fig. 3** Co-added video frames (with enhanced contrast) showing the spectra of meteors 1, 3, 4 and 6. In all cases the meteor flew from upper left to bottom right and the wavelengths increase from bottom left to upper right. The main emissions are identified. There is a small gap in the data of meteor 4 due to tape failure.

The plots of the other six spectra are given in Fig. 5. These spectra have much lower signal-to-noise ratio than spectra 4 and 6. Nevertheless, the intensities of Mg, Na, and Fe (multiplet 15) lines could be measured (except for meteor 2, where only the red part of the spectrum was captured). These lines have been used by Borovička et al. (2005) to compare the content of Mg, Fe, and Na in meteoroids of various origin. As it can be seen in Fig. 6, the Draconids fall in the region of meteors with normal, i.e. chondritic, composition. Other studies (Millman 1972; Borovička et al. 2007; Madiedo et al. 2013) also concluded that the ratios of major elements are chondritic in Draconids. Madiedo et al. (2013) gave also the abundances of minor elements but their values are based on low resolution and noisy spectra and cannot be considered as reliable.

Another aspect is the temporal evolution of the spectra. The previous studies (Millman 1972; Borovička et al. 2007) noted a shift of the Na line toward higher altitudes in some Draconids. This was also the case of a  $-10$  mag fireball (Madiedo et al. 2013). Interestingly, our two best spectra 4 and 6 are quite different in this respect (Figs. 3 and 7). Meteor 4 is a pronounced example of the early start and early end of the sodium line. The maximum of Na is shifted up by about 5 km in comparison with Mg. In meteor 6, Na is present along the whole trajectory in nearly constant proportion to Mg. Though both meteoroids had almost the same initial mass (Table 2), the heights of the maxima and the shapes of the light curves were also quite different (Figs. 1 and 7). Meteor 4 had a flat maximum around height 95 km, while meteor 6 exhibited a bright flare at a much lower height of 83 km. All these facts suggest that the meteoroid structure may be different.

**Table 4** Identification of spectral features in meteor 6.

No.	Observed		Atom-Multiplet	Identified Wavelengths	2nd order
	Wavelength	Intensity			
1	3810w	100	Fe I - 20 Mg I - 3 Fe I - 4 Fe I - 45	3820, 3826, 3834 3838, 3832, 3829 3860, 3856, 3824 3816	
2	4250w	35	Fe I - 42 Ca I - 2 Cr I - 1	4326, 4308, 4272 4227 4254, 4275	
3	4380	55	Fe I - 41 Fe I - 2	4384, 4405 4376	
4	4450	40	Fe I - 2	4427, 4462, 4482	
5	4570	12	Mg I - 1	4571	
6	4700	9	Mg I - 11	4703	
7	4970w	9	Fe I - 318	4958, 4920	
8	5110	14	Fe I - 1	5110	
9	5180	70	Mg I - 2 Fe I - 1	5184, 5172, 5167 5166, 5169	
10	5260	18	Fe I - 15	5270	
11	5330	12	Fe I - 15	5328	
12	5420	14	Fe I - 15	5405–5456	
13	5530	5	Mg I - 9	5528	
14	5580	5	Fe I - 686 Ca I - 21	5615, 5586, 5572 5588, 5594	
15	5890	100	Na I - 1	5890, 5896	
16	6200–6800		N <sub>2</sub> 1st. positive		
17	7000–7500		N <sub>2</sub> 1st. positive		
18	7460	7	N I - 3	7468, 7442, 7424	
19	7690	16	K I - 1	7665, 7699	Mg I - 3, Fe I - 4
20	7770	60	O I - 1	7772, 7774, 7775	
21	8210	40	N I - 2 Na I - 4	8185–8223 8195, 8183	
22	8470	20	O I - 4	8446	Ca I - 2

Wavelengths are given in Å; "w" means wide line. Intensities are in relative units, taking into account the spectral sensitivity of the instrument. The continuum and molecular emissions were subtracted from the intensities. Saturation of bright lines was taken into account. Only the most important second order contributors are listed.

## 5 Deceleration

In order to get more insight into the structure of the meteoroids, we evaluated their decelerations along the trajectory. In fact, the directly measured quantity is the position of the meteor as a function of time (or frame number). Of course, individual position measurements are subject to error. Moreover, once fragmentation starts, the meteor is no longer a point-like object. As drag depends on mass, grains of different sizes separate along the meteor's direction of travel to form a streak of light (Borovička et al. 2007; Campbell-Brown et al. 2013). As the fragmentation and ablation proceeds, different parts of the streak may become the brightest part. This effect may lead to large scatter of apparent deceleration/acceleration from frame to frame. Thus, as a first step, we evaluated the lag of each meteor along its trajectory. The lag at any time is defined as the difference between the predicted meteor position in case of zero deceleration (i.e. considering only the initial position and velocity) and the actual position. Since the time is a relative quantity for each meteor, meteors are best

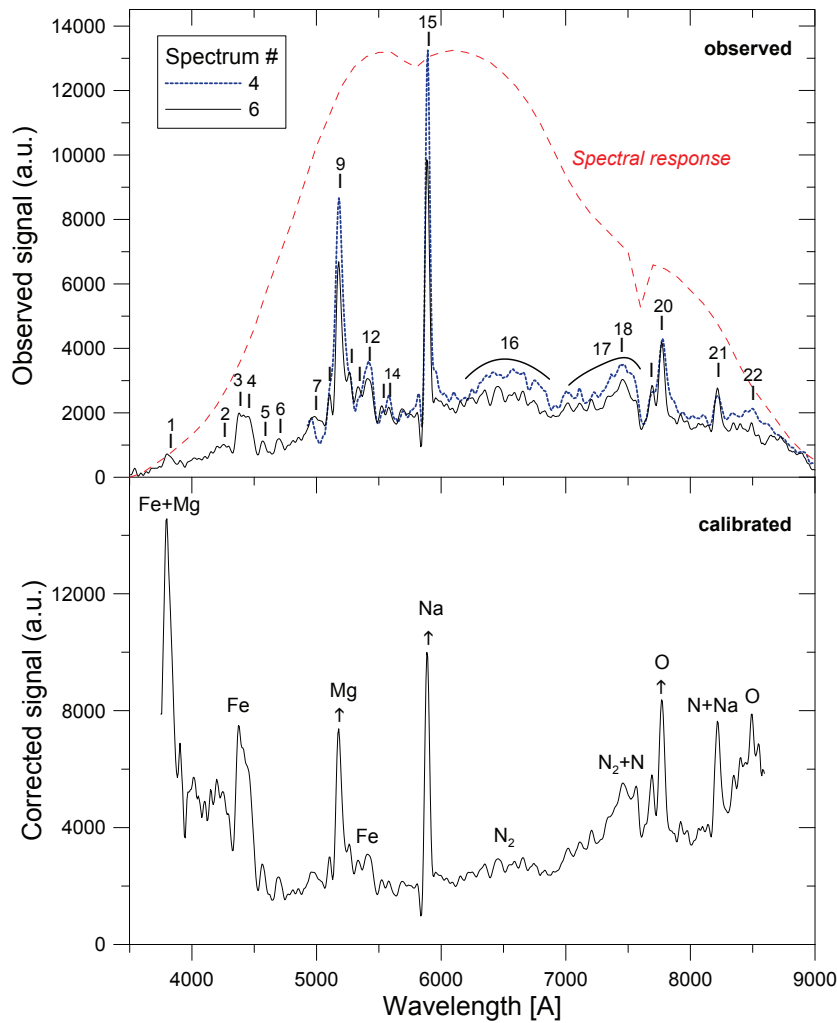


**Fig. 4** Line identifications in Draconid meteor spectra. The upper panel shows the observed signal, integrated along the trajectory, as a function of wavelength for meteors 4 and 6. The blue part of spectrum 4 was outside the field of view. The spectral features identified in Table 4 are marked. Note that the intensity of the three strongest lines (9, 15, 20) is underestimated in the figure due to saturation during the meteor maximum. The dashed line shows the relative spectral response of the system, measured using stellar spectra. The dip at 7600 Å is due atmospheric O<sub>2</sub> absorption. The lower panel shows spectrum 6 after correction to the spectral response. The intensity above 7500 Å was affected by the admixture of second order spectrum. The minimum just left of the Na line is an artifact.

compared by the lag as a function of predicted height. The predicted height is the height as it would be without deceleration.

The comparison of the lag of meteors 4 and 6 is given in Fig. 8. We can see that the lag (and thus the deceleration) was much larger for meteor 4 than for meteor 6. This is another substantial difference between these two meteors, besides the shape of the light curve and the release of sodium, and again suggests differences in structure and fragmentation history.



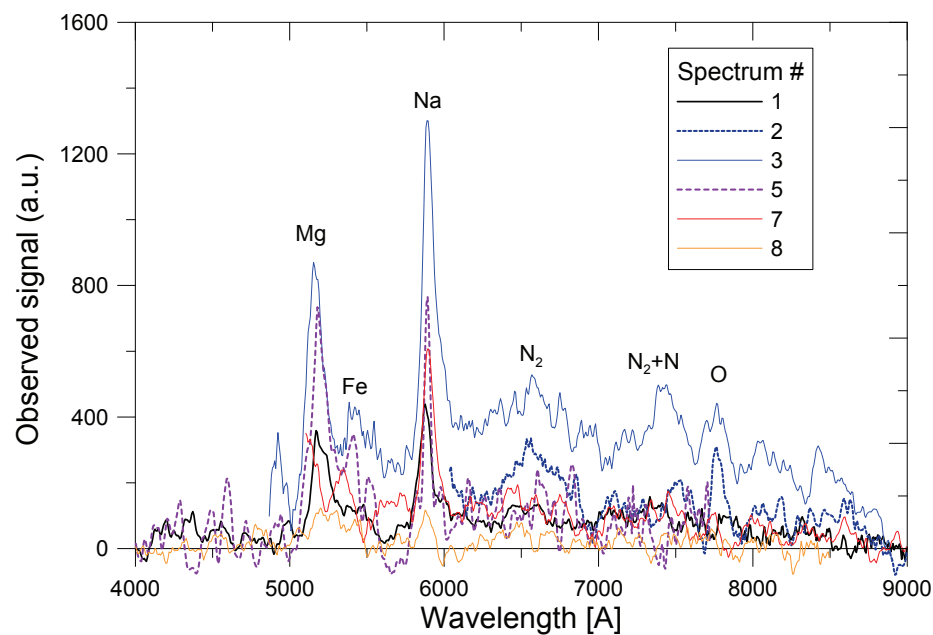


**Fig. 5** Fainter Draconid spectra. Observed signal, integrated along the trajectory, is given as a function of wavelength. The noise caused some curves to fall below zero after the background was subtracted.

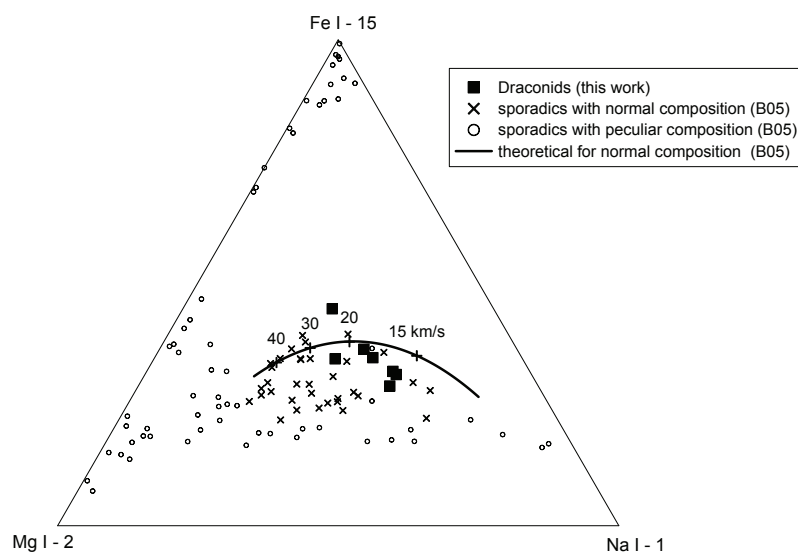


**Fig. 6** Ternary diagram comparing the time-integrated intensities of Mg, Na, and Fe multiplets in meteor spectra. Draconids studied in this work are plotted together with sporadic meteors studied by Borovička et al. (2005, =B05). Meteors classified by that work as having normal (i.e. chondritic) Mg-Fe-Na ratios are distinguished from meteors with various peculiarities. A theoretical curve for thermal equilibrium showing the expected positions of normal meteors as a function of their velocity is also shown (Borovička et al. 2005).

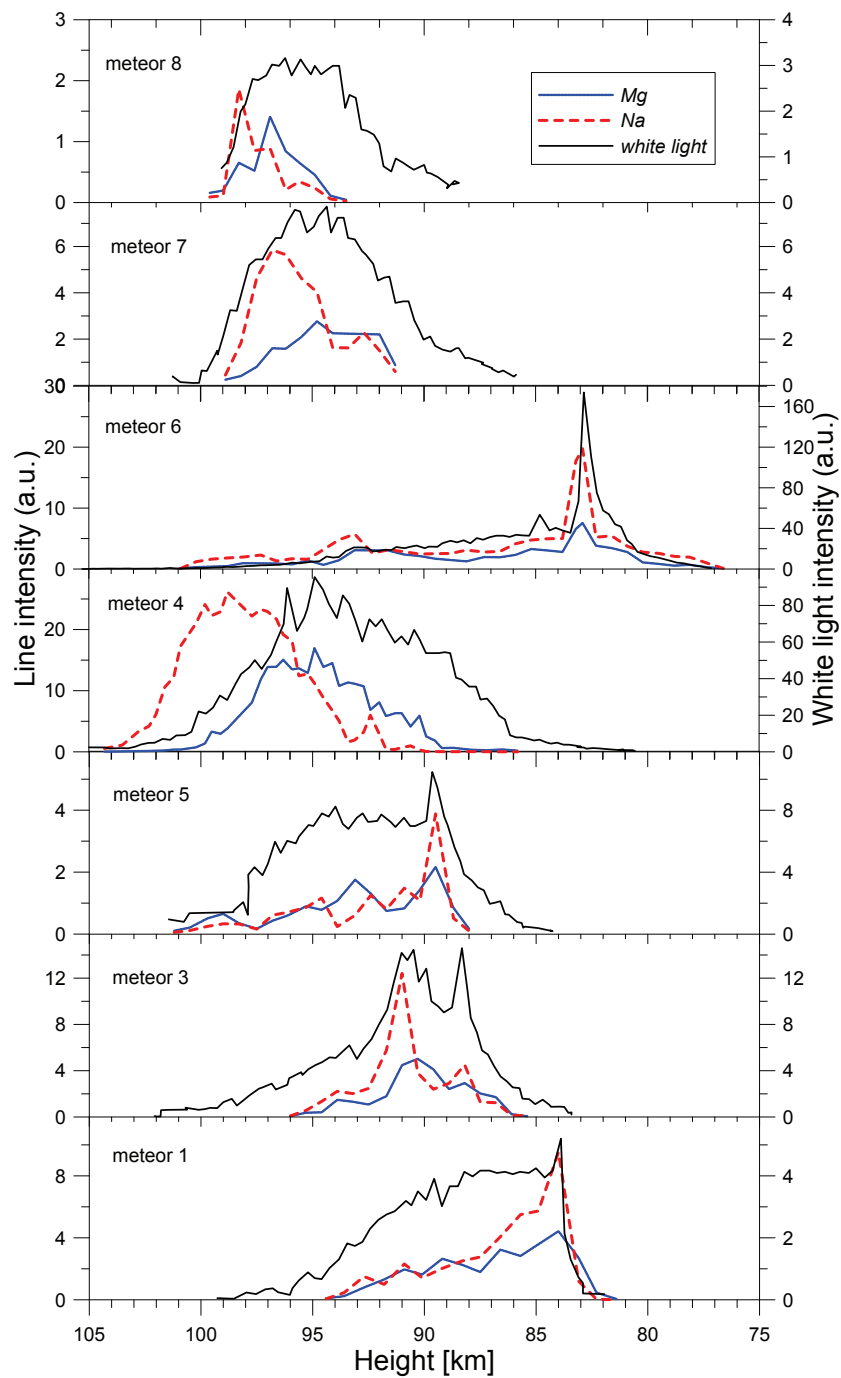


**Fig. 7** Monochromatic light curves in the Mg and Na lines compared to the total light curves in white light. The intensities are in relative linear scale. The scale in white light is different compared to the Mg and Na lines because the total intensity was measured on non-spectral cameras. The order of the plots was adjusted to facilitate direct comparison of meteors 4 and 6. Heights for the spectral curves are known to a precision of 1 km or better.

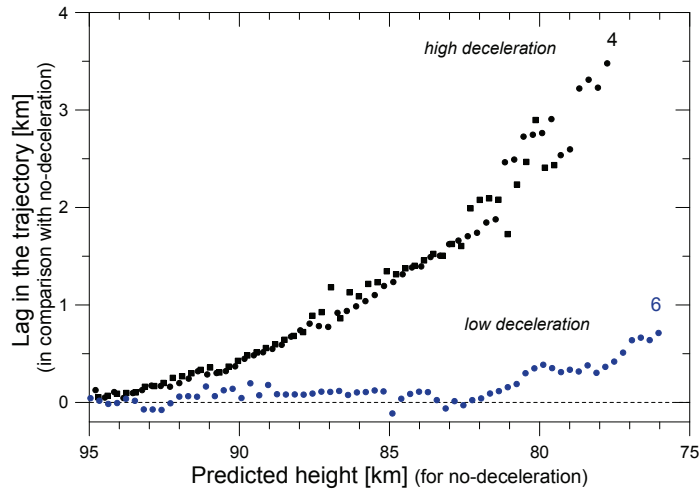


**Fig. 8** Measured lag along the trajectory between the predicted position in case of no-deceleration and the actual position as a function of predicted height for meteors 4 and 6. Different symbols for meteor 4 represent the measurements from two different sites.

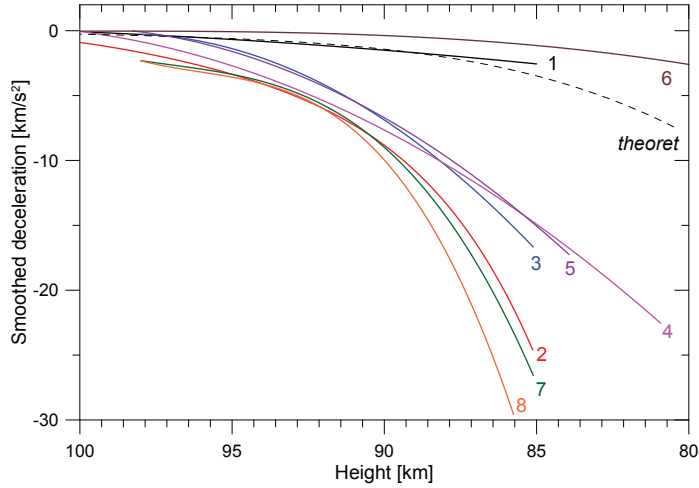


**Fig. 9** Deceleration of eight Draconid meteors, smoothed by the erosion model, as a function of height. The dashed line labeled *theoret* shows the expected deceleration of a non-fragmenting spherical Draconid meteoroid of a mass of  $10^{-4}$  kg, bulk density  $200 \text{ kg m}^{-3}$  (diameter 1 cm), ablation coefficient  $0.02 \text{ s}^2 \text{ km}^{-2}$  and zenith angle  $22^\circ$ . Meteor 6 showed less deceleration because it was more massive.

The erosion model, described in detail by Borovička et al. (2007), can provide further insight into the causes of the differences between individual Draconid meteors. The model assumes that a gradual continuous release of individual grains, from which the meteoroid is composed, starts at a certain height, after the meteoroid received a certain amount of energy per unit surface from the collisions with atmospheric molecules. After the release, each grain behaves as an individual meteor. The grain density is assumed to be  $3000 \text{ kg m}^{-3}$ . The bulk density of the whole meteoroids can be much lower due to high porosity. The rate of the grain release is described by the erosion coefficient,  $\eta$ . The rate of ablation (vaporization)

**Table 5** Selected parameters of the erosion model fits.

#	$E_S$ MJ/m <sup>2</sup>	$f$	$\eta$ s <sup>2</sup> /km <sup>2</sup>	$\sigma$ s <sup>2</sup> /km <sup>2</sup>	$h_{es}-h_{ee}$ km	Sizes $\mu\text{m}$	$E_S$ (2) MJ/m <sup>2</sup>	$\eta$ (2) s <sup>2</sup> /km <sup>2</sup>	S (2) $\mu\text{m}$
1	1.9	0.83	0.30	0.022	96–86	110	16	0.8	5
2	0.4	1.00	3.5	0.024	105–97	130			
3	1.5	0.50	0.6	0.027	98–94	170	4.2	0.7	80
4	0.5	1.00	2.3	0.015	105–93	150–30			
5	0.9	0.86	0.7	0.032	101–91	200–40	6.3	0.8	60
6	1.1	0.84	0.15	0.015	101–78	130–20	23	1.0	5
7	1.2	1.00	1.0	0.014	100–94	100–20			
8	1.4	1.00	1.0	0.019	100–95	100–20			

$E_S$  is the energy received per unit cross-section before the erosion starts;  $f$  is the fraction of mass of the meteoroid subject to the initial erosion;  $\eta$  and  $\sigma$  are the erosion and ablation coefficients, respectively;  $h_{es}-h_{ee}$  is the height range of the initial erosion; Sizes is the size range of grains. Values designated with (2) apply to the second stage erosion.

of both the grains and the whole meteoroid is described by the ablation coefficient,  $\sigma$ . The erosion may proceed in several (usually two) stages, i.e. the initial erosion may be applied only to a certain percentage of the meteoroid, while the rest continues unaffected (only subject to ablation) for some more time. The parameters of the erosion model are adjusted to fit the light curve in white light and the lag in the trajectory.

To provide some deceleration data, we smoothed the lag data fits obtained with the erosion model (Borovička et al. 2007) and plotted the corresponding decelerations in Fig. 9. Only meteors 1 and 6 exhibited low deceleration. We can see the decelerations of these two meteors were not higher than expected for non-fragmenting meteoroids of very low bulk density ( $\sim 200 \text{ kg m}^{-3}$ ) and similar mass.

Table 5 gives the most important parameters of the erosion fits. The most fragile meteoroids 2 and 4 were characterized by an early start of erosion, high erosion rate, and the fact that their whole mass was subject to the initial erosion (although these meteoroids were among the largest in our sample). Meteoroids 1 and 6 were characterized by much slower grain release, so that the erosion was finished only at heights much lower than 90 km. Moreover, about 1/6 of both meteoroids did not participate in the initial erosion and resisted fragmentation to lower heights (84 and 83 km, respectively). Here they disrupted abruptly into very small grains. On the other hand, there was no clear trend in grain sizes and ablation coefficients among the eight meteors. We also computed the bulk densities but they are uncertain at least by a factor of two. The obtained bulk densities were between 100–200  $\text{kg m}^{-3}$  for meteors 2, 3, 7, and 8 and between 350–450  $\text{kg m}^{-3}$  for meteors 1, 4, 5, and 6. These differences may not be real; nevertheless, the erosion model confirms that Draconids are meteoroids with low bulk densities.

## 6 Meteor morphologies

Besides light curves and decelerations, meteor morphologies, i.e. the shapes of meteor images, are indicative of the fragmentation process (Campbell-Brown et al. 2013). With high resolution, individual fragments can be imaged or meteor wakes caused by differential deceleration of grains can be measured. We got high resolution images of meteor 6 with our non-intensified HDV camera. They are compared with the images from the low resolution but high sensitivity MAIA camera in Fig. 10. Meteor height marks have been added to the

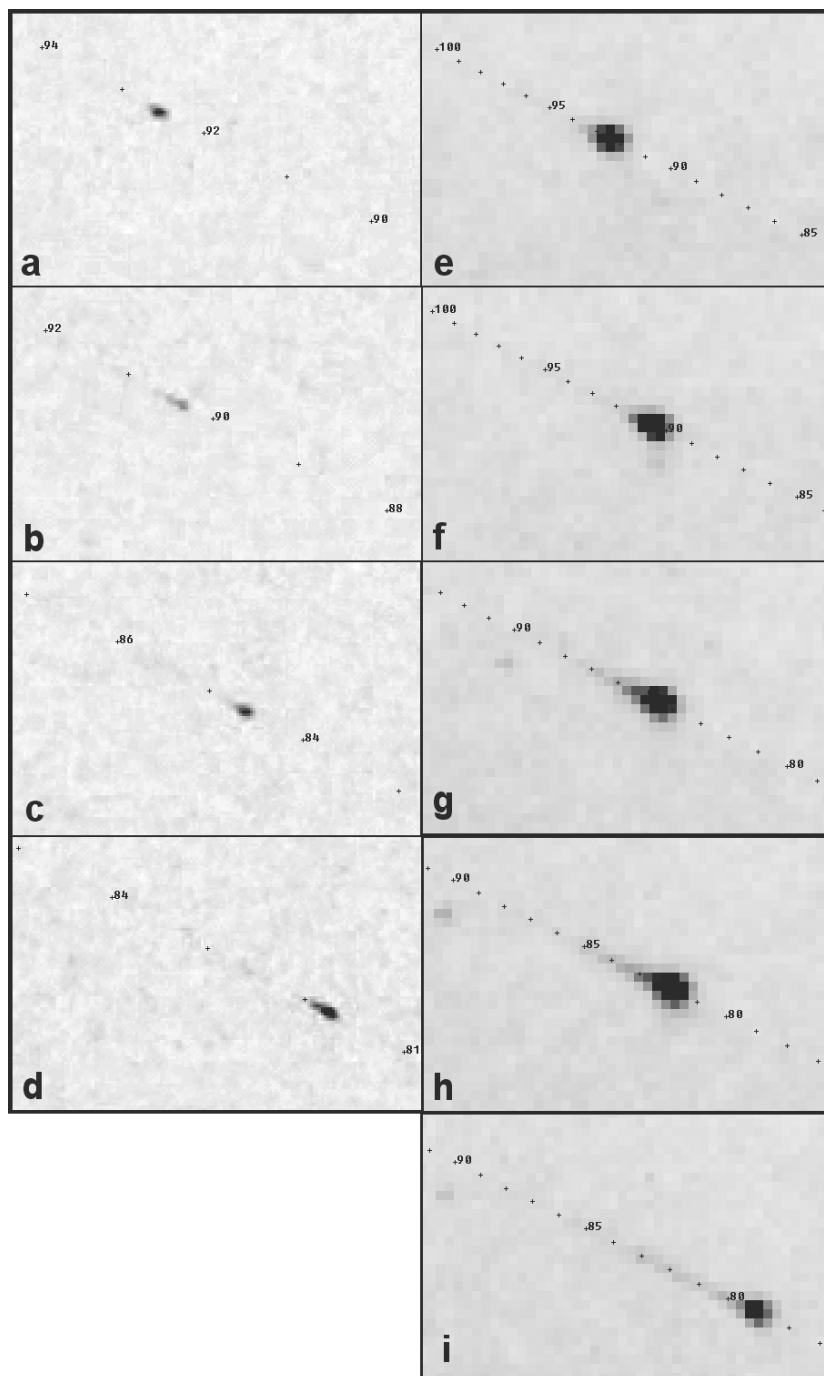


**Fig. 10** Inverted images of meteor 6 at the heights 92.5, 90.5, 84.5, and 82 km from the HDV camera (panels a-d) and the nearly corresponding images from the MAIA camera (panels e-h). The image from the MAIA camera at the height 79 km is shown in panel i. The meteor was too faint for the HDV camera at that height. Height marks in the step of 1 km are given for the scale.

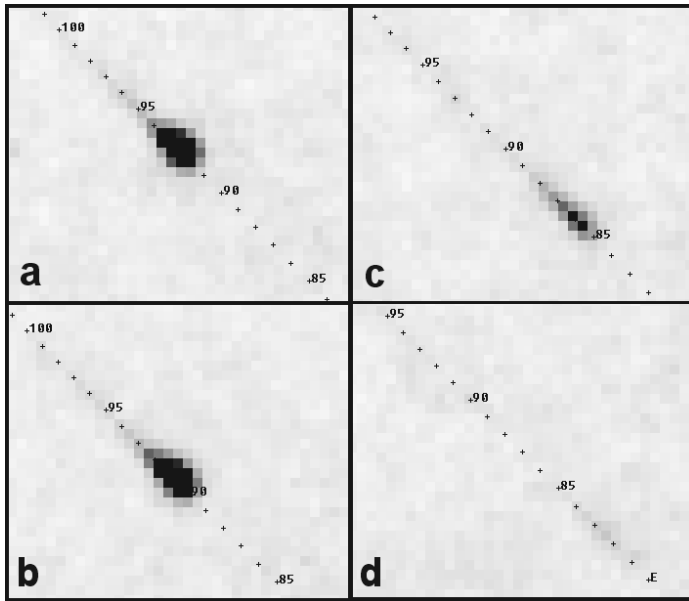


**Fig. 11** Inverted images of meteor 4 at the heights 92, 90, 85, and 82 km from the MAIA camera. Height marks in the step of 1 km are given for the scale.

images from both cameras. The HDV camera provides the shape of the brightest part of the meteor, which was too bright and unresolved on the MAIA images. For comparison, the images of meteor 4 from the MAIA camera are presented in Fig. 11.

We can see that meteor 6 was still nearly point-like at the height of 92.5 km and only slightly elongated at 90.5 km. At 84.5 km, the meteor head was quite concentrated again but there was a faint wake seen in the MAIA camera, about 2 km long. At 82 km, both the head and the wake became longer. At 79 km, the wake was more than 6 km long but the meteor head was still well defined. Meteor 4 was clearly elongated in the low resolution MAIA image already at the height of 92 km and the elongation increased with time. At lower heights, the meteor became a streak of light without any head. These differences are consistent with our interpretation that meteoroid 4 quickly disintegrated into grains, which dispersed along the trajectory. Meteoroid 6 fragmented more slowly and in two stages. We note that the long wake may not have been caused only by the ablating grains, since Draconids also exhibit persistent trains (Trigo-Rodríguez et al. 2013) whose radiation is driven by different mechanisms (Borovička 2006a).

## 7 Discussion

We have combined spectroscopy, photometry, dynamics and morphology of Draconid meteors to study physical and chemical properties of the meteoroids from comet 21P/Giacobini-Zinner. The meteoroids were somewhat larger (sizes 1 – 3 cm) than the majority of meteoroids from our previous Draconid study (Borovička et al. 2007). The spectra were not available in the previous study, except for one bright Draconid.

Meteors 2, 4, 7, 8 had some common characteristics: smooth and flat light curves without any flares, high decelerations, and the release of most sodium in the first half of their trajectories (at least meteors 4, 7, 8 – we do not have complete spectrum of meteor 2). All these features can be explained by the complete and quick disintegration of the meteoroids into small grains. In our model, the disintegration was finished at the height of 93 km or larger for all four meteors. At the disintegration end height, almost all the sodium had evaporated. We believe that the reason was that the grains were small enough to release sodium and potassium from their whole volumes earlier than the other elements were vaporized, an effect called differential ablation (Janches et al. 2009). Alternatively, sodium may be part of a hypothetical glue which holds the grains together (Hawkes & Jones 1975).

Meteors 1 and 6 exhibited flares at relatively low heights 84–83 km, where other Draconids had nearly disappeared. The deceleration of meteoroids 1 and 6 was much lower and sodium was present along the whole trajectories. Our analysis suggests that their bulk density was not very different from the meteoroids of the previous group and their fragmentation started at similar heights or only somewhat lower. The main difference was that either the grain release was much slower or they fragmented in a somewhat different manner. Moreover, significant parts of the meteoroids (1/6 of mass in both cases) resisted the fragmentation until heights of 84–83 km. Here they disrupted abruptly causing the meteor flares. These more compact parts contained significant sodium and the sodium was radiated out efficiently during the flares (see Fig. 7). It is possible that mechanical strength of the material was exceeded at these heights, where the dynamic pressure reached 5 kPa. This would still mean a quite low mechanical strength in comparison with most non-Draconid meteoroids (Borovička 2006b).

Meteoroids 3 and 5 were intermediate cases. The light curves and the sodium release pattern were similar to meteors 1 and 6 but the decelerations were higher and the flares occurred at larger altitudes. Meteoroid 3 was particularly complex since it exhibited three stages of erosion/fragmentation.

We note that meteors 1 and 2, which may have come from an older ejection event than the others, have very different characteristics, and are each more similar to meteors from the main peak than to each other. This fact suggests that the differences found among the meteoroids reflect the inhomogeneity of the cometary material and not the exposure age in space.

## 8 Conclusions

We analyzed eight moderately bright Draconid meteors. Some of the most precise trajectories and orbits of the 2011 Draconids were provided. The main purpose of this work was, nevertheless, to study the physical and chemical properties of Draconid meteoroids. Our data are consistent with the known fact that Draconids are porous conglomerates of grains and the abundance ratios of the main elements (Mg, Fe, Na) are chondritic. Nevertheless, significant differences in fragmentation behavior of cm-sized Draconids were found. Various textures with various resistance to atmospheric fragmentation clearly exist among Draconid meteoroids and even within single meteoroids.

**Acknowledgements** We thank the other expedition participants, Jaroslav Boček and Vlastimil Vojáček, for their assistance. Pavel Spurný navigated us remotely to the clear sky region. Karel Fliegel and Stanislav Vítek prepared the MAIA cameras. We thank the referees, Margaret Campbell-Brown, Edward Stokan, and an anonymous referee, for their comments and improvements of the text. This work was supported by

grants P209/11/1382 and P209/11/P651 from GA ČR. System MAIA was developed within the GA ČR grant 205/09/1302. The institutional project was RVO:67985815.

## References

- J. Borovička, Meteor trains – terminology and physical interpretation. *J. R. Astron. Soc. Canada* **100**, 194–198 (2006a)
- J. Borovička, Physical and chemical properties of meteoroids as deduced from observations. In: *Asteroids, Comets, and Meteors* (eds.: D. Lazzaro, S. Ferraz-Mello, J.A. Fernandez), Cambridge Univ. Press. Proceedings IAU Symposium No. **229**, pp. 249–271 (2006b)
- J. Borovička, R. Štork, J. Boček, First results from video spectroscopy of 1998 Leonid meteors. *Meteorit. Planet. Sci.* **34**, 987–994 (1999)
- J. Borovička, P. Koten, P. Spurný, J. Boček, R. Štork, A survey of meteor spectra and orbits: evidence for three populations of Na-free meteoroids. *Icarus* **174**, 15–30 (2005)
- J. Borovička, P. Spurný, P. Koten, Atmospheric deceleration and light curves of Draconid meteors and implications for the structure of cometary dust. *Astron. Astrophys.* **473**, 661–672 (2007)
- J. Borovička, P. Koten, L. Šrbený, R. Štork, K. Hornoch, Radiants, orbits, spectra, and deceleration of selected 2011 Draconids. In Gyssens M. and Roggemans, P., editors, *Proceedings of the International Meteor Conference, La Palma, 20–23 September 2012*, pp. 65–69 (2013)
- M. D. Campbell-Brown, J. Vaubaillon, P. Brown, R. J. Weryk, R. Arlt, The 2005 Draconid outburst. *Astron. Astrophys.* **451**, 339–344 (2006)
- M. D. Campbell-Brown, J. Borovička, P. G. Brown, E. Stokan, High-resolution modelling of meteoroid ablation. *Astron. Astrophys.* **557**, A41, 13pp. (2013)
- R. L. Hawkes, J. Jones, A quantitative model for the ablation of dustball meteors. *Mon. Not. R. Astron. Soc.* **173**, 339–356 (1975)
- D. Janches, L. P. Dyruud, S. L. Broadley, J. M. C. Plane, First observation of micrometeoroid differential ablation in the atmosphere. *Geophys. Res. Lett.* **36**, id L06101 (2009)
- P. Jenniskens, *Meteor Showers and their Parent Comets*. Cambridge Univ. Press, 790pp. (2006)
- J. Kero, Y. Fujiwara, M. Abo, C. Szasz, T. Nakamura, MU radar head echo observations of the 2011 October Draconids. *Mon. Not. R. Astron. Soc.* **424**, 1799–1806 (2012)
- P. Koten, J. Borovička, P. Spurný, R. Štork, Optical observations of enhanced activity of the 2005 Draconid meteor shower. *Astron. Astrophys.* **466**, 729–735 (2007)
- P. Koten, K. Fliegel, S. Vitek, P. Páta, Automatic video system for continues monitoring of the meteor activity. *Earth Moon Planets* **108**, 69–76 (2011)
- J. M. Madiedo, J. M. Trigo-Rodríguez, N. Konovalova, I. P. Williams, A. J. Castro-Tirado, J. L. Ortiz, J. Cabrera-Caño, The 2011 October Draconids outburst – II. Meteoroid chemical abundances from fireball spectroscopy. *Mon. Not. R. Astron. Soc.* **433**, 571–580 (2013)
- M. Maslov, Future Draconid outbursts (2011 – 2100). *WGN, Journal of the IMO* **39**, 64–67 (2011)
- P. M. Millman, Giacobinid Meteor Spectra. *J. R. Astron. Soc. Canada* **66**, 201–211 (1972)
- P. Pecina, Z. Ceplecha, New aspects in single-body meteor physics. *Bull. Astron. Instit. Czechoslovakia* **34**, 102–121 (1983)
- J. Tóth, R. Piffel, J. Koukal, P. Žołądek, M. Wiśniewski, Š. Gajdoš, F. Zanotti, D. Valeri, P. De Maria, M. Popek, S. Gorková, J. Világi, L. Kornoš, D. Kalmančok, P. Zigo, Video observation of Draconids 2011 from Italy. *WGN, Journal of the IMO* **40**, 117–121 (2012)



- J. M. Trigo-Rodríguez, J. M. Madiedo, I. P. Williams, J. Dergham, J. Cortés, A. J. Castro-Tirado, J. L. Ortiz, J. Zamorano, F. Ocaña, J. Izquierdo, A. Sánchez de Miguel, J. Alonso-Azcárate, D. Rodríguez, M. Tapia, P. Pujols, J. Lacruz, F. Pruneda, A. Oliva, J. Pastor Erades, A. F. Marín, The 2011 October Draconids outburst – I. Orbital elements, meteoroid fluxes and 21P/Giacobini-Zinner delivered mass to Earth. *Mon. Not. R. Astron. Soc.* **433**, 560–570 (2013)
- J. Vaubaillon, J. Watanabe, M. Sato, S. Horii, P. Koten, The coming 2011 Draconids meteor shower. *WGN, Journal of the IMO* **39**, 59–63 (2011)
- J. Vaubaillon, P. Koten, R. Rudawska, S. Bouley, L. Maquet, F. Colas, J. Tóth, J. Zender, J. McAuliffe, D. Pautet, P. Jenniskens, M. Gerding, J. Borovička, D. Koschny, A. Leroy, J. Lecacheux, M. Gritsevich, F. Duris, Overview of the 2011 Draconids airborne observation campaign. In Gyssens M. and Roggemans, P., editors, *Proceedings of the International Meteor Conference, La Palma, 20–23 September 2012*, pp. 61–64 (2013)